Biotransformation of cyclocanthogenol by the endophytic fungus *Alternaria eureka* 1E1BL1

Güner Ekiz [a], Seda Duman [b], Erdal Bedir [b, *]

[a] *Department of Pharmacognosy, Faculty of Pharmacy, Near East University, Nicosia, Mersin 10, Turkey*
[b] *Department of Bioengineering, Faculty of Engineering, Izmir Institute of Technology, 35430 Urla-Izmir, Turkey*

ABSTRACT

The microbial transformation of cyclocanthogenol (CCG), *Astragalus* sp. originated sapogenin, by the endophytic fungus *Alternaria eureka* 1E1BL1 isolated from *Astragalus angustifolius* was investigated. Hydroxylation, oxidation, epoxidation, *O*-methylation, ring-expansion and methyl migration reactions were observed on the triterpenoid skeleton. As a result, eight metabolites were isolated and the structures of the previously undescribed compounds were established by 1-D, 2-D NMR and HR-MS analyses.

© 2018 Elsevier Ltd. All rights reserved.

1. Introduction

Biotransformation is chemical modifications that occur when enzymes or whole cell systems are used as catalysts (Borges et al., 2009; de Carvalho, 2011, 2016). This is a useful method for production of new potent molecules, overcoming the problems associated with chemical synthesis reactions/enhancement of the productivity and providing the basic information needed to elucidate the biosynthetic pathways. Producing large amounts of biomass and having great enzyme diversity with chemo-, regio- and enantio-selective catalytic abilities make microbial systems logical choice for biotransformation studies (Carballeira et al., 2009; Pimentel et al., 2011; Tao and Xu, 2009). Whole-cell biocatalysis is expected to play a significant role in this growing area of pharmaceutical industry (Lam, 2009). According to the literature, microbial transformation is one of the most commonly used method for transformation of saponins to obtain more active derivatives (Shah et al., 2014; Vincken et al., 2007). Filamentous fungi have been one of the most studied whole cell systems for biotransformation reactions. Recently, endophytic fungi have received great attention due to their ability to transform complex natural products with a high degree of stereospecificity. Considering the fact that endophytes continuously interact with their hosts via special enzymes and chemicals, they may be promising source of biocatalyst with numerous application (Bianchini et al., 2015; Borges et al., 2009; Ludwig-Müller, 2015; Wang and Dai, 2011). However, utilization of the plants' own endophytes to transform plants' own secondary metabolites have been scarcely explored in the field of biotransformation.

The genus *Astragalus* (Fabaceae) is one of the richest sources of cycloartanes, the unique triterpenoids with a characteristic 9,19-cyclopropane ring. Cycloartane-type saponins from *Astragalus* species have exhibited wide range of biological activities including wound healing, immunomodulatory, antineoplastic, hepatoprotective, antimutagenic, antiviral and antiprotozoal activities (Çalış et al., 1997; Özipek et al., 2005; Nalbantsoy et al., 2011). Cycloastragenol, the main sapogenol of many cycloartane-type glycosides found in *Astragalus* genus, has attracted great attention as a telomerase activator which was discovered in a systematic screening studies of natural product extracts from traditional Chinese medicines (Harley et al., 2010).

Not only potency of cyloartanes as telomerase activators but also the absence of endophytic fungi's utilization in biotransformation

prompted us to make an attempt to generate a chemical library. In continuation of our previous efforts (Kuban et al., 2010, 2013; Tağ et al., 2012; Bedir et al., 2015), we performed microbial transformation on *Astragalus* cycloartanes by using endophytic fungi isolated from *Astragalus* species. In this study, cyclocanthogenol (CCG), one of the major sapogenins in *Astragalus* genus, was subjected to biotransformation by fungal endophyte *Alternaria eureka* (Pleosporaceae) 1E1BL1. Herein, we report isolation and structural elucidation of eight (**1**−**8**) biotransformation products with diverse chemistry.

2. Results and discussion

A total of 15 endophytic fungi, isolated from the roots, stems and leaves of *Astragalus* plants, were screened by TLC for their ability to transform CCG into previously undescribed derivatives. Based on the preliminary screening results, the endophytic isolate identified as *Alternaria eureka* 1E1BL1 was selected for further biotransformation studies. Analytical scale biotransformation was performed to determine the optimal harvesting time of the fungus for transformation of the starting compound. Preparative scale biotransformation of CCG with *A. eureka* 1E1BL1 for 10 days yielded seven previously undescribed metabolites **1**−**7**, along with the known compound **8** (Fig. 1). The structures of **1**−**8** were characterized by HR-MS, 1D-, and 2D-NMR data.

Compounds **1**, **2** and **3** were monohydroxylated products of CCG.

The HR-MS data of compound **1** (m/z 531.3664 [M+Na]$^+$, calcd for $C_{30}H_{52}O_6Na$, 531.3661) supported a molecular formula $C_{30}H_{52}O_6$, implying a monohydroxylation of the starting compound. In the ^1H NMR spectrum, the AX system signals of cyclopropane ring, seven methyl groups in the up-field region, and the characteristic signals belonging to the H-3, H-6, H-16 and H-24 oxymethine protons in the low-field displayed no significant discrepancy compared to CCG. Apart from the characteristic low-field signals, an additional oxymethine signal at δ 3.82 was observed corresponding to a carbon at δ 73.7 in the HSQC spectrum. The ^{13}C NMR spectrum of **1** showed that C-11 (δ 39.7) and C-13 (δ 50.5) signals had undergone a significant down-field shift (*ca.* 16 and 5 ppm, respectively) when compared to that of CCG, suggesting a hydroxylation at C-12 position. This assumption was confirmed with the long-distance correlations in the HMBC spectrum from δ 3.82 to C-13, C-14 and C-18, and H-11 and H-18 to δ 73.7. In order to establish the stereochemistry at C-12, a 2D-NOESY experiment was performed. The nOe correlation between H-12 and β-oriented H$_3$-18 indicated the α-configuration of 12-OH. On the basis of these results, the structure of **1** was established as 3β,6α,12α,16β,24(*S*),25-hexahydroxycycloartane.

The HR-MS spectrum of **2** showed a major ion peak at m/z 531.3679 [M+Na]$^+$ ($C_{30}H_{52}O_6Na$). Like **1**, compound **2** displayed the 9,19-cyclopropane ring signals of CCG, seven methyl groups, and the signals belonging to the H-3, H-6, H-16 and H-24 oxymethine protons. The signal observed at δ 4.04 suggested another
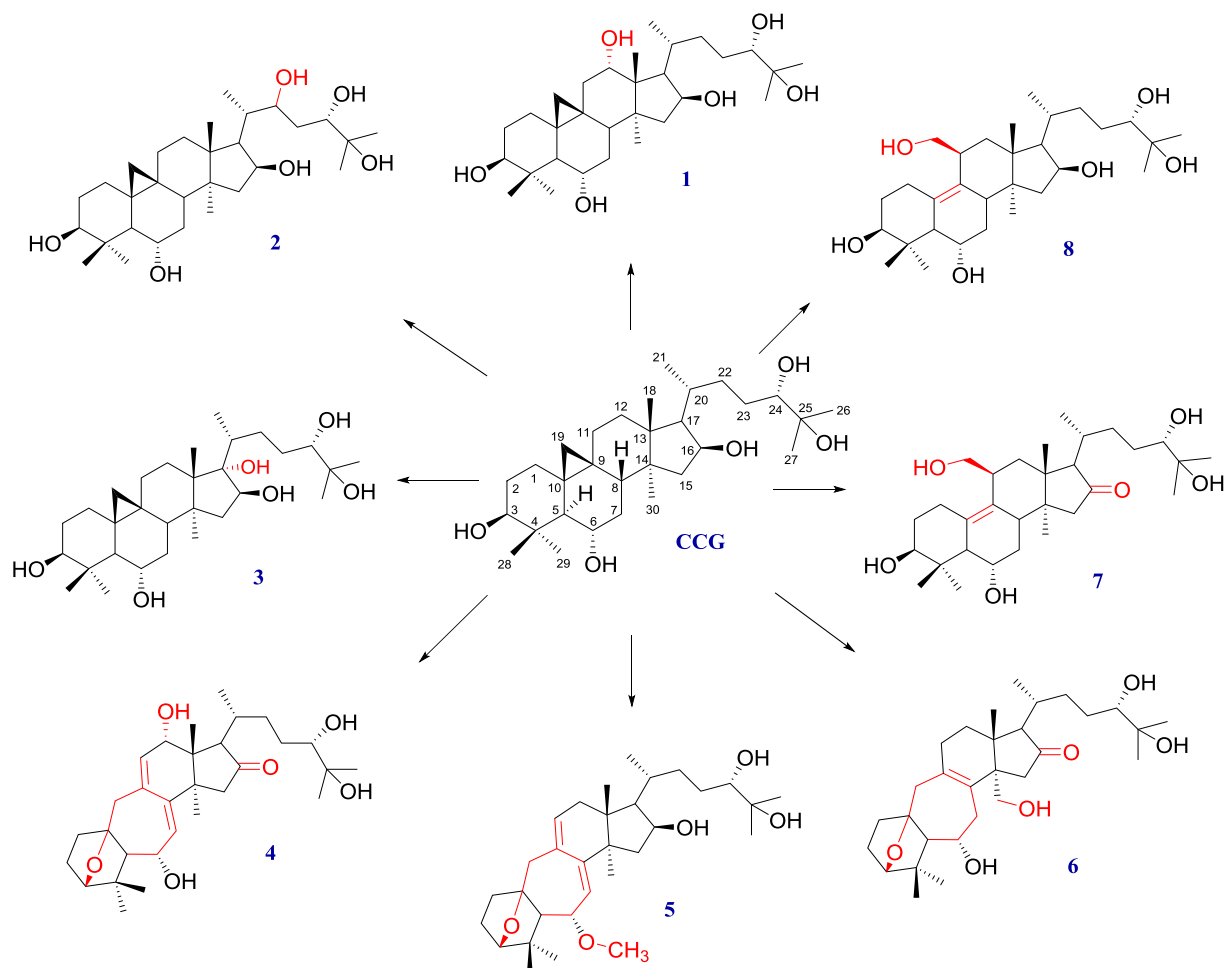

Fig. 1. Transformation products of cyclocanthogenol (CCG).

oxymethine group corresponding to a carbon at δ 75.3 in the HSQC spectrum. A detailed inspection of the ^{13}C NMR spectrum showed down-field shift for C-20 and C-23 signals (ca. 12 ppm) when compared to that of CCG, therefore, a hydroxylation at C-22 was suggested. In the COSY spectrum, the partial identification of the side-chain spin system starting from the distinct H-24 proved this suggestion [H-24 (δ 3.53 dd, J = 10.5, 2.2 Hz) → H$_2$-23 (1.58 m, 1.77 m) → H-22 (δ 4.04 dd, J = 7.3, 5.8 Hz)] (Fig. 2). Furthermore, the key long correlations observed in the HMBC spectrum from H-22 to C-24, and from H-21/H$_2$-23 to C-22 justified the hydroxylation at C-22. Based on the NOESY data, one of the intriguing observation in the COSY spectrum was missing $^3J_{H-H}$ coupling between H-22 and H-20. This data implied that somehow the side chain was not freely rotating to adopt different conformers setting the dihedral angle of the H-20/C-20/C-22/H-20 system to be about 90°. Therefore it was proposed that the conformational flexibility was prohibited due to a couple of hydrogen bond formations in a hydroxyl group rich vicinity (C-16, C-22, C-24 and C-25). To confirm this hypothesis and stereochemistry of C-22, minimized energy conformers of **2** were calculated by MM2 molecular mechanics program. Although an appropriate dihedral bond angle was reached with 22(S) absolute configuration revealing hydrogen bonds between side chain OH groups [C-22(OH)/C24(OH) and C-24(OH)/C25(OH)], the observed ROESY correlations did imply free rotation in the side chain. The determination of the configuration of the stereocenter C-22 was not possible. On the basis of these results, the structure of **2** was established as 3β,6α,16β,22,24(S),25-hexahydroxycycloartane.

The HR-MS data of compound **3** (m/z 531.3672 [M+Na]$^+$, calcd for C$_{30}$H$_{52}$O$_6$Na, 531.3661) displayed 16 amu increase over the starting compound, implying monohydroxylation. The signals of 9,19-cyclopropane ring and seven methyl groups, and H-3, H-6, H-16 and H-24 resonances were observed readily in the ^{1}H NMR spectrum as in **1** and **2**. In the ^{13}C NMR spectrum, apart from the C-3, C-6, C-16, C-24 and C-25 oxygenated carbons, an additional signal at δ 89.3 was observed. In the HSQC spectrum, no correlation of this carbon with any proton indicated its quaternary nature. The δ 89.3 resonance was unambiguously assigned to C-17 based on the long-distance correlations in the HMBC from H-16, H-15a, H$_3$-18 and H$_3$-21 protons to δ 89.3 (Fig. 3). Additionally, down-field shifts of C-16, C-14 and C-20 signals substantiated the hydroxylation position. A thorough literature search on biotransformation metabolites of the steroidal compounds proposed a single configuration for C-17(OH) to be alpha. However, to establish the orientation unambiguously, NMR spectrum of **3** was recorded in pyridine-d_5 to observe the exchangeable proton of C-17(OH). Based on the $^3J_{C-H}$ HMBC correlations between the exchangeable proton at δ 4.83 (s) and C-16/C-13, 17(OH) was readily located. In the 2D-ROESY spectrum, cross peaks from this exchangeable proton to the axial H-12α
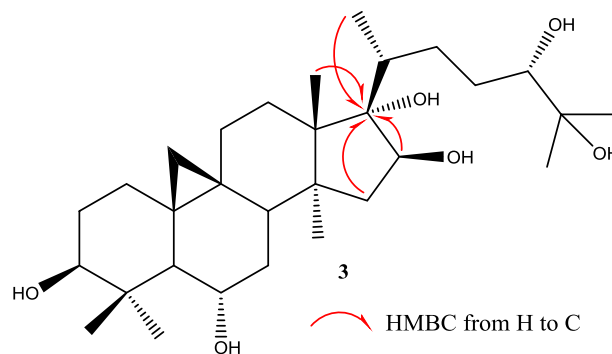

Fig. 3. Key long-range correlations (HMBC) of **3**.

proton (δ 2.58, t, 11.8 Hz), and from the latter to H$_3$-30 exhibited that all these protons were cofacial with alpha orientation. Thus, the structure of **3** was identified as 3β,6α,16β,17α,24(S),25-hexahydroxycycloartane.

The molecular formula of compound **4** was established as C$_{30}$H$_{46}$O$_6$ by HR-MS analysis (m/z 525.3206 [M+Na]$^+$, calcd for C$_{30}$H$_{46}$O$_6$Na, 525.3192). In the ^{1}H NMR spectrum, the disappearance of the AX system signals deriving from 9,19-cyclopropane ring suggested a ring cleavage. The hydroxymethine proton at C-16 was not present in the ^{1}H NMR spectrum. In addition, a new doublet signal at δ 4.03 was observed together with two olefinic protons (δ 5.46 and 5.68). In the ^{13}C NMR spectrum, apart from the C-3, C-6, C-24 and C-25 oxygenated carbons, two additional signals at δ 72.3 and 88.3 were detected. The ^{13}C NMR spectrum of **4** also exhibited four olefinic carbon resonances (δ 128.4, 134.2, 136.8 and 141.8) and a carbonyl signal at δ 221.4. The combined use of DQF-COSY and HSQC spectra, allowed the assignment of two spin systems (Fig. 2): 'A' (H-3 → H$_2$-1) and 'B'(H-5 → H$_2$-19). The spin system A includes the H-3 resonance (δ 3.73 d, J = 5.6 Hz) which showed correlation with H-2b (δ 1.74 m), while the latter proton showed cross peak with H-2a (δ 2.00 m), which, in turn, coupled with both H$_2$-1 protons (δ 1.38 m and 1.58 m). The second spin system (B) includes a methine proton at δ 1.61 (m, H-5) which showed correlation with the oxymethine proton at C-6 (δ 4.54 dd, J = 10.3, 3.4 Hz) and from there to an olefinic methine proton at δ 5.46 (dd, J = 3.5, 1.3 Hz, H-7). The H-7 proton showed $^5J_{H-H}$ coupling with H-11 through the conjugated double bond system (δ 5.68 d, J = 5.5 Hz) in the DQF-COSY spectrum. H-11 coupled with oxymethine proton at δ 4.03 (d, J = 6.0 Hz, H-12) which, in turn, exhibited cross peaks with the H$_2$-19 methylene protons (δ 2.67 d, J = 14.3 Hz; δ 3.04 d, J = 14.0 Hz). Location of the olefinic double bonds was assigned from the correlations in the HMBC spectrum. The two signals (δ 2.67 and 3.04)
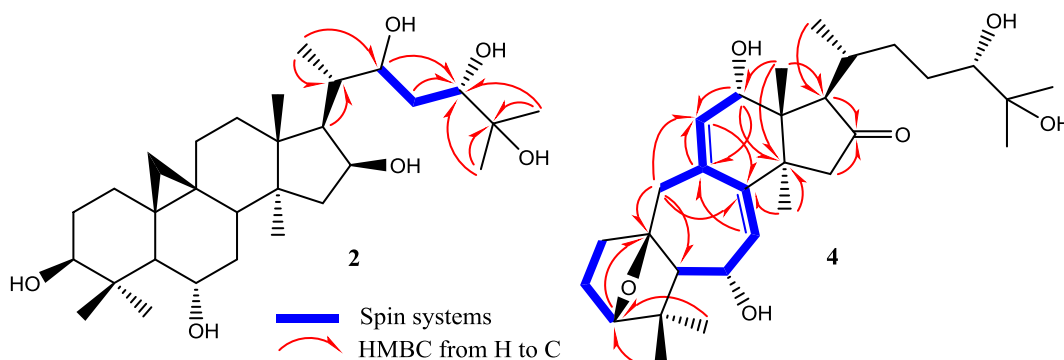

Fig. 2. The partial spin systems (COSY) and key long-range correlations (HMBC) of **2** and **4**.

were assigned to H_2-19 based on the long-distance correlations in the HMBC spectrum (δ 2.67 to C-5, C-10, C-11, C-9 and C-8; δ 3.04 to C-10, C-11 and C-9) indicating a seven-membered B ring resulting from the cleavage of the cyclopropane ring. The long-distance correlations from H_2-19, H-12 and H-7 to the quaternary carbon at δ 134.2 revealed the location of the double bond between C-9 and C-11. The other trisubstituted double bond was positioned between C-7 and C-8 based on the HMBC correlations from H-19b, H-11 and H_3-30 to the quaternary 141.8 ppm signal. Additionally, the carbon signal at δ 221.4 displayed long-range correlations with the protons of H_2-15 and H-17, implying the oxidation of C-16 secondary alcohol to a ketone. On the other hand, a new signal observed at δ 4.03, corresponding with a carbon at 72.3 ppm in the HSQC spectrum, indicated an additional oxymethine group. The HMBC spectrum showed long-distance correlations from δ 4.03 proton to C-9, C-11, C-14. Based on these findings, the new hydroxyl group was located at C-12. The hydroxyl group at C-12 was deduced to be α-oriented on the basis of ROESY correlation of H-12 (δ 4.03) with the beta oriented H_3-18 (δ 0.84). The carbon signal at 86.8 ppm had long-range correlations with H_3-28 and H_3-29 in the HMBC spectrum, readily assigned to C-3. Additionally, downfield shift of C-3 signal suggested that an oxygen bridge involving C-3 atom was present in the framework. Resemblance of the spectral data of **4** with those of previously reported compounds (Feng et al., 2015) together with the long-distance correlation of the quaternary carbon at 88.3 ppm with H-3 (δ 3.73) provided evidence for the oxygen bridge between C-3 and C-10 carbons. The orientation of 3(10)-epoxy bridge was confirmed by inspecting the ROESY spectrum of **4** and calculating its minimized energy conformer by MM2 molecular mechanics program. In the ROESY spectrum, H-3 showed strong correlation with H_3-28 (δ 1.22), which in turn correlated with H-6β. Moreover, a weak nOe correlation between H-3 and H_3-29 was observed. The minimized energy conformer of **4** clearly showed that β-oriented 3(10)-epoxy bridge above the A ring made H-3 to lie in close proximity with H_3-28 (2.45 Å) instead of alpha oriented H_3-29 (2.9 Å) (*see* Supplementary information: Fig. S36). For the alpha-oriented epoxy bridge, completely conflicting interatomic distances with the ROESY correlations were measured, revealing 3(10)β-epoxy bridge. Thus, **4** was deduced to be 6α,12α,24(*S*),25-tetrahydroxy-3(10)β-epoxy-9,10-seco-cycloartane-7,9(11)-dien-16-one.

The compound **5** had a molecular formula of $C_{31}H_{50}O_5$ based on the HR-MS data (*m/z* 525.3566 [M+Na]$^+$, calcd for $C_{31}H_{50}O_5Na$, 525.3555). An additional carbon suggested the insertion of a methyl group into the structure. When 1D NMR spectra of **5** were inspected, their similarities with those of **4** were acknowledged at once. Major differences between these two compounds were that the signals for the oxymethine at C-12 and the ketone resonance of C-16 in **4** were missing, instead, additional signals for *O*-methyl group (δ_H = 3.33 and δ_C = 56.5) were observed in **5** together with hydroxylated C(H)-16 resonances as in the case of **1**. The methoxy protons at δ 3.33 showed an HMBC correlation with δ 79.2 (C-6), suggesting that *O*-methylation occurred at C-6. Therefore, **5** was identified as 16β,24(*S*),25-trihydroxy-6α-methoxy-3(10)β-epoxy-9,10-seco-cycloartane-7,9(11)-diene.

The HR-MS spectrum of **6** (*m/z* 527.3370 [M+Na]$^+$, calcd for $C_{30}H_{48}O_6Na$, 527.3348) supported a molecular formula of $C_{30}H_{48}O_6$. The absence of 9,19-cyclopropane ring signals in the ^{1}H NMR spectrum suggested a ring cleavage as in **4** and **5**. Five tertiary methyl group signals observed in the up-field region, implying a modification on one of the methyl groups compared to the starting compound. An AB system at δ 3.50 and 3.76 confirmed the presence of a primary alcohol group. In the ^{13}C NMR spectrum, apart from the already expected carbon signals, two oxygen-bearing methine carbons (δ 68.7 and 89.1), two olefinic carbons (δ 131.2 and 132.5)

and a ketone carbonyl signal (δ 221.9) were observed in the low-field region. In the HSQC spectrum, no correlation were observed between any protons with the carbons at δ 131.2 and 132.5, justifying a tetrasubstituted olefinic system. These olefinic signals were attributed to C-9 and C-8, respectively, according to the HMBC correlations from H-7, H-12 and H-19 to the signal at δ 131.2, and from H-7 and H-30 to δ 132.5 resonance. The ^{3}J-HMBC correlations of the oxymethylene protons at δ 3.50 and 3.76 with the C-8, C-14 and C-15 signals revealed the position of oxygenated methyl at C-30. Finally, the HMBC correlation between H-15 with the carbon resonance at δ 221.9 confirmed the location of the ketone group to be C-16. As a result, the structure of **6** was established as 6α,24(*S*),25,30-tetrahydroxy-3(10)β-epoxy-9,10-seco-cycloartane-8(9)-en-16-one.

The molecular formula of **7** was established as $C_{30}H_{50}O_6$ by HR-MS analysis (*m/z* 529.3522 [M+Na]$^+$, calcd for $C_{30}H_{50}O_6Na$, 529.3505). In the ^{1}H NMR spectrum, the signals of a cyclopropyl ring were not detected, implying a ring cleavage. In addition, the hydroxymethine proton at C-16 was lost in the ^{1}H NMR spectrum compared to the starting compound. In the ^{13}C NMR spectrum, a signal observed at δ 68.8 correlated with two proton resonances at δ 3.51 and 3.44 (AB system) in the HSQC spectrum, indicating the presence of an oxymethylene group. On the other hand, a carbonyl signal at δ 221.8 was noticed from the ^{13}C NMR spectrum together with two olefinic carbon signals (δ 132.3 and 136.6). In the HSQC spectrum, no correlations of any protons with the olefinic carbons indicated a tetrasubstituted olefinic system. The double bond was located between C-9 and C-10 on the basis of the HMBC correlations from H-1 and H-5 to the δ 132.3 signal, as well as from H-1 to the δ 136.6 signal. Furthermore, the HMBC correlation between H_2-12 and C-19 suggested that the cyclopropane methylene carbon (C-19) migrated over to C-11. The similarity between the spectral data of **6** and previously reported biotransformation products of cycloartanes not only supported our assumption but also helped us to deduce the relative stereochemistry of C-19 to be β (Kuban et al., 2010, 2013; Yang et al., 2012). Additionally, the long-range correlations of H_2-15 and H-17 with the carbonyl carbon at δ 221.8 confirmed the oxidation of C-16(OH) to a ketone. Consequently, metabolite **7** was deduced to be 3β,6α,16β,19,24(*S*),25-hexahydroxy-ranunculan-9(10)-en-16-one.

The ^{1}H and ^{13}C NMR spectra of **8** were in agreement with those reported for 3β,6α,16β,19,24(*S*),25-hexahydroxy-ranunculan-9(10)-ene, previously obtained from the biotransformation study of CCG with *Cunninghamella blakesleeana* NRRL 1369 (Bedir et al., 2015).

3. Conclusion

Despite their promising potential as biocatalysts, the use of plant-associated endophytic fungi to transform plant originated secondary metabolites have been scarcely explored. After preliminary screenings, microbial transformation studies were carried out using 15 endophytic fungi isolated from different parts of *Astragalus* plants. Based on the analytical scale results, *Alternaria eureka* 1E1BL1, a fungal species never exploited as a biocatalyst, was selected for further biotransformation studies. Preparative scale incubation of CCG with this endophytic fungus afforded eight metabolites (**1–8**). *A. eureka* 1E1BL1 was found to be capable of hydroxylation, oxidation, epoxidation, *O*-methylation, ring-expansion and methyl migration reactions on the cycloartane nucleus. These modifications resulted in the formation of the compounds that would be difficult or impossible to prepare by conventional synthetic methods.

Compounds **1**, **2** and **3** were monohydroxylated analogs of CCG having hydroxyl groups at C-12, C-17 and C-22 positions, respectively, produced by P450-catalyzed monooxygenation reactions.

Unusually, the fungus did monohydroxylate CCG at C-17 and C-22 positions. The presence of a hydroxyl group at aforementioned positions has been rarely reported in the literature for triterpenoidal saponins (Lu et al., 2010; Shaymaa et al., 2016; Yoshikawa et al., 2000). To the best of our knowledge, 17- and 22-hydroxylation of cycloartane nucleus by microbial transformation was never reported.

Apart from the monohydroxylation reactions, *A. eureka* 1E1BL1 catalyzed ring expansion and epoxidation reactions on CCG (**4**, **5** and **6**) to form 3(10)β-epoxy-9,10-seco-cycloartane structure. The microbial-catalysis of the B ring expansion reactions have been observed in the transformation of cycloastragenol to give 9,10-seco-cycloartane skeleton by the fungus *Syncephalastrum racemosum* AS 3.264 (Feng et al., 2015; Yang et al., 2012). However, a reaction mechanism was not proposed for this unique biotransformation. In Fig. 4, a tentative reaction pathway is shown for compounds **4**—**6**. As cyclopropane ring behaves like a double bond in nature, C-1, C-5, C-8 and C-11 positions are subject to allylic rearrangements. A hydrogen abstraction from C-11 or C-8 by P450 enzyme results in carbocation formation, which in turn leads to migration of C-9/C-10 bond of the cyclopropane ring to yield a seven membered ring (9,10-seco-cycloartane), C-8(C-9) or C-9(C-11) double bond and a carbocation at C-10 position. As a result of this transformation, the ring A favors boat conformation, which rearranges C-3(OH) and C-10 to lie in close proximity (*ca.* 1.9—2.0 Å, calculated by minimized energy conformers). This adjacent localization facilitates the nucleophilic attack of C-3(OH) to the carbocation (C-10) to give 3(10)β-epoxy framework.

In addition, compounds **7** and **8** were the rearrangement products of CCG resulting from the cleavage of 9,19-cyclopropane ring followed by methyl migration. This unique transformation was reported previously in the biotransformation of CA and CCG by *Cunninghamella blakesleeana* NRRL 1369, *Syncephalastrum*

racemosum AS 3.264 and *Alternaria alternata* AS 3.4578 (Bedir et al., 2015; Feng et al., 2015; Kuban et al., 2010; Yang et al., 2012).

Consequently, this is the first report in *Astragalus* sapogenin chemistry utilizing *Astragalus* originated endophytic fungi. The results of this study prove that biotransformation using endophytic fungi is an efficient tool for the structural modification of secondary metabolites to expand compound libraries and prediction of tentative mammalian metabolites of traditionally used crude drugs.

4. Experimental

4.1. General experimental procedures

Mass spectrometry experiments were carried out on an Agilent 1200/6530 Instrument − HRTOFMS. NMR spectra were recorded on Varian Oxford AS400 and Bruker DRX-500 instruments. The chemical shifts were measured relative to the residual solvent peak and are expressed in δ (ppm) and the coupling constant (*J*) are reported in Hertz (Hz). Silica gel 60 (70−230 mesh, Merck), Sephadex LH-20 (GE Healthcare Life Sciences) and RP-18 (Chromabond C18, Macherey-Nagel) were used for column chromatography. TLC analyses were carried out on Silica gel 60 F254 (Merck) and RP-18 F254s (Merck) plates. Spots were visualized under UV light and by spraying with 20% H_2SO_4/water reagent followed by heating at 105 °C for 1−2 min.

4.2. Plant material and the starting compound

Astragalus angustifolius and *Astragalus condensatus* (Fabaceae) were collected from Spil Mountain (38° 33.965' N, 27° 24.400' E), Manisa, Turkey in June 2013, and identified by Serdar Gökhan Şenol (Department of Biology, Faculty of Science, Ege University, Turkey). The plant samples were put into plastic bags and transported to the
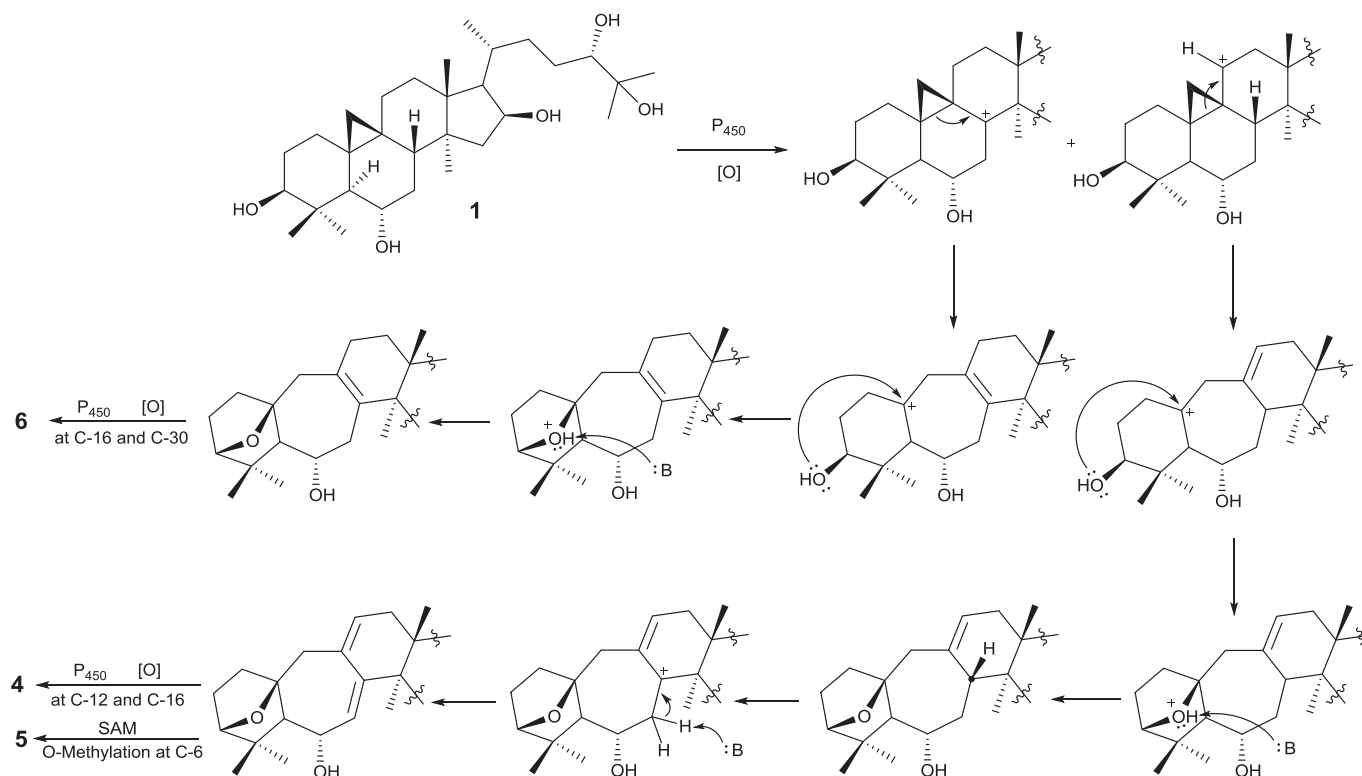

Fig. 4. The plausible mechanism for the transformation of compounds **4**, **5** and **6**.

laboratory within 24 h. The starting compound, cyclocanthogenol (CCG), was donated by Bionorm Natural Products Ltd. (İzmir, Turkey).

4.3. Fungal material

The fungal endophytes used in this study were isolated from fresh and healthy tissues of *Astragalus* species. The plant samples were washed thoroughly in running tap water followed by distilled water to remove any dirt and the adhering soil particles. Then, the plant materials were cut into small pieces and were subjected to surface sterilization under aseptic condition. The samples were surface-sterilized by sequential immersion in 70% ethanol for 5 min, %3−5 sodium hypochlorite for 5 min, and 70% ethanol for 30 s. Finally, the surface-sterilized plant tissues were rinsed in sterile distilled water three times for 1 min, then air dried under a laminar-flow hood. The outer tissues were removed from the air-dried plant samples with the help of a flame-sterilized scalpel and the inner tissues were cut into small fragments. The tissue fragments were then placed in Petri dishes containing potato dextrose agar (PDA), malt extract agar (MEA), Rose-Bengal Chloramphenicol (RBC) agar and water agar (WA) and incubated at 25 °C until fungal growth started. To confirm the success of surface sterilization procedure, 100 μL aliquots of water from the last washing step were inoculated on PDA and incubated under the same conditions in parallel. The plates were monitored every day to check the growth of endophytic fungi. The hyphal tips that emerged from the tissue fragments were isolated and subcultured onto PDA

media. Subsequently, the pure fungal cultures were transferred on PDA slants and stored at 4 °C.

The endophytic fungus 1E1BL1 was identified by the identification service at Deutsche Sammlung von Mikroorganismen und Zellkulturen GmbH (DSMZ), Braunschweig, Germany. The identification of the fungal isolate was done on the basis of the sequence of rDNA ITS, which is the first common DNA-barcode for fungi (Schoch et al., 2012). Additionally, amplification and sequencing of the large subunit of rDNA (LSU) and the TEF1 gene were performed (Woudenberg et al., 2013). The assembled DNA sequences were compared with those in GenBank, MycoID and various databases as well as with the type species of *Alternaria eureka* (Pleosporaceae).

4.4. Microbial transformation procedures

The microbial transformation process was conducted at two scales; analytical and preparative. One-stage fermentation protocol was followed where CCG was fed to the biotransformation media 72 h after the inoculation (Kuban et al., 2010). On analytical scale, the mycelial agar plugs (8 mm in diameter) from 5-day-old fungal cultures grown on PDA plate were inoculated into 250 ml Erlenmeyer flask containing 50 ml biotransformation medium (2% glucose, 0.5% yeast extract, 0.5% NaCl, 0.5% Na_2HPO_4, 0.5% peptone (w/v)) adjusted to pH 6.0. After inoculation, the flasks were incubated on a rotary shaker at 180 rpm, 25 °C for 72 h. CCG (10 mg dissolved in 500 μl of DMSO) was added to 72-h-old cultures, which were then incubated at 25 °C, 180 rpm for 21 days. The samples were taken on days 0, 2, 4, 7, 10, 14, 17, 21 and centrifuged at

Table 1
^{1}H NMR data of metabolites **1–7** (400 MHz, in CD_3OD).

H	1	2	3	4	5	6	7
	δ_H(ppm), *J* (Hz)	δ_H(ppm), *J* (Hz)	δ_H(ppm), *J* (Hz)	δ_H(ppm), *J* (Hz)	δ_H(ppm), *J* (Hz)	δ_H(ppm), *J* (Hz)	δ_H(ppm), *J* (Hz)
1	1.28 m, 1.66 m	1.26 m, 1.58 m	1.25 m, 1.57 m	1.38 m, 1.58 m	1.32 m, 1.49 m	1.45 m, 1.76 m	1.83 m, 2.31 d (14.4)
2	1.62 m, 1.74 m	1.61 m, 1.70 m	1.61 m, 1.71 m	1.74 m, 2.00 m	1.72 m, 1.97 m	1.67 m, 2.05 m	1.47 m, 1.88 m
3	3.23 dd (10.8, 4.6)	3.32 dd (10.9, 4.4)	3.22 dd (4.4, 10.9)	3.73 d (5.6)	3.72 d (5.6)	3.83 d (7.4)	3.36 dd (4.5, 11.2)
4							
5	1.34 m	1.33 m	1.34 d (9.9)	1.61 m	1.57 d (10.6)	1.50 d (9.6)	1.80 m
6	3.41 m	3.45 dt (9.8, 3.3)	3.44 m	4.54 dd (10.3, 3.4)	4.05 dd (10.3, 2.8)	3.69 td (10.1, 2.7)	3.76 ddd (11.6, 7.2, 4.5)
7	1.35 m, 1.41 m	1.38 m, 1.46 m	1.35 m, 1.41 m	5.46 dd (3.5, 1.3)	5.36 brs.	2.21 m, 2.57 m	1.35 m, 1.57 m
8	1.64 m	1.81 dd (12.1, 3.9)	1.78 m				2.45 d (10.9)
9							
10							
11	1.75 dd (9.3, 13.3), 2.0 dd (13.3, 5.1)	1.19 m, 1.99 m	1.16 m, 2.09 m	5.68 d (5.5)	5.47 brs.	2.20 m, 2.27 m	3.04 m
12	3.82 dd (3.9, 5.9)	1.65 m (2H)	1.44 m, 2.11 m	4.03 d (6.0)	2.18 brs. (2H)	1.95 m, 2.20 m	1.51 m, 1.86 m
13							
14							
15	1.41 m, 2.02 m	1.43 m, 2.04 m	1.41 m, 2.15 dd (13.2, 8.5)	2.10 d (17.7), 2.45 d (17.6)	1.74 m, 2.10 dd (12.9, 8.1)	2.46 s (2H)	1.97 d (19.7), 2.19 d (18.4)
16	4.46 ddd (5.4, 7.9, 7.9)	4.46 ddd (5.6, 7.6, 7.6)	4.19 dd (5.8, 8.2)		4.55 ddd (5.6, 7.7, 8.0)		
17	2.30 dd (11.0, 7.8)	2.08 m		2.94 d (7.3)	1.70 m	2.72 m	2.37 d (7.1)
18	1.10 s	1.18 s	1.23 s	0.84 s	0.87 s	1.07 s	1.07 s
19	0.47 d, 0.50 d (4.5)	0.38 d (4.3), 0.53 d (4.1)	0.43 d (4.2), 0.51 d (4.2)	2.67 d (14.3), 3.04 d (14.0)	2.55 d (13.9), 3.02 d (13.6)	2.29 d (14.9), 2.75 d (14.8)	3.51 dd (10.7, 5.0), 3.44 t (11.1)
20	1.92 m	2.11 m	2.04 m	1.73 m	1.94 m	1.84 m	1.76 m
21	1.07 d (6.6)	0.92 d (6.4)	0.94 d (6.0)	1.09 d (6.8)	0.97 d (6.4)	1.09 d (6.8)	1.06 d (6.8)
22	1.43 m, 1.82 m	4.04 dd (7.3, 5.8)	1.29 m, 1.71 m	1.56 m, 1.90 m	1.23 m, 1.80 m	1.59 m, 1.92 m	1.78 m, 2.74 m
23	1.29 m, 1.61 m	1.58 m, 1.77 m	1.41 m, 1.62 m	1.41 m, 1.59 m	1.43 m, 1.63 m	1.45 m, 1.64 m	1.39 m, 1.58 m
24	3.40 m	3.53 dd (10.5, 2.2)	3.40 m	3.30 m	3.38 dd (10.9, 1.9)	3.36 m	3.28 m
25							
26	1.15 s	1.16 s	1.15 s	1.15 s	1.15 s	1.21 s	1.14 s
27	1.17 s	1.22 s	1.16 s	1.17 s	1.17 s	1.24 s	1.17 s
28	1.24 s	1.22 s	1.24 s	1.22 s	1.15 s	1.20 s	1.17 s
29	0.95 s	0.95 s	0.96 s	1.12 s	1.07 s	1.18 s	0.68 s
30	1.02 s	0.99 s	1.28 s	1.32 s	0.97 s	3.50 d (11.4), 3.76 d (11.4)	0.96 s
1′					3.33 s		

Table 2
^{13}C NMR data of metabolites **1**–**7** (100 MHz, in CD$_3$OD).

C	1 δ_C (ppm)	2 δ_C (ppm)	3 δ_C (ppm)	4 δ_C (ppm)	5 δ_C (ppm)	6 δ_C (ppm)	7 δ_C (ppm)
1	33.7 t	33.5 t	33.5 t	38.8 t	38.5 t	40.3 t	31.9 t
2	31.1 t	31.1 t	31.1 t	25.8 t	25.7 t	26.5 t	32.8 t
3	79.4 d	79.5 d	79.4 d	86.8 d	86.8 d	87.9 d	78.4 d
4	42.7 s	42.7 s	42.7 s	48.3 s	48.0 s	46.5 s	42.5 s
5	54.6 d	54.5 d	54.7 d	63.6 d	62.8 d	64.9 d	57.8 d
6	70.3 d	69.8 d	70.3 d	68.9 d	79.2 d	68.2 d	68.5 d
7	39.3 t	38.9 t	39.3 t	136.8 d	130.5 d	40.7 t	37.4 t
8	49.6 d	48.8 d	51.0 d	141.8 s	145.7 s	132.5 s	40.9 d
9	22.0 s	22.2 s	22.2 s	134.2 s	132.8 s	131.2 s	132.3 s
10	30.7 s	30.7 s	31.1 s	88.3 s	88.6 s	89.1 s	136.6 s
11	39.7 t	27.0 t	27.4 t	128.4 d	127.6 d	30.76 t	39.3 d
12	73.7 d	34.0 t	28.0 t	72.3 d	39.3 t	30.82 t	33.7 t
13	50.5 s	47.8 s	51.6 s	48.7 s	45.0 s	47.0 s	42.7 s
14	47.3 s	46.5 s	47.1 s	46.9 s	50.9 s	51.0 s	46.5 s
15	50.2 t	48.5 t	49.3 t	49.8 t	45.3 t	42.1 t	49.8 t
16	73.2 d	73.1 d	82.5 d	221.4 s	72.8 d	221.9 s	221.8 s
17	49.8 d	53.3 d	89.3 s	57.2 d	57.0 d	62.7 d	63.2 d
18	18.5 q	19.2 q	21.0 q	18.6 q	17.2 q	19.2 q	18.1 q
19	32.3 t	31.8 t	32.6 t	41.5 t	41.4 t	39.1 t	68.8 t
20	29.4 d	35.4 d	35.7 d	32.8 d	30.0 d	33.0 d	32.7 d
21	16.0 q	13.4 q	14.2 q	18.5 q	18.6 q	19.6 q	19.5 q
22	33.8 t	75.3 d	30.5 t	33.6 t	33.8 t	33.9 t	29.4 t
23	28.5 t	34.9 t	29.2 t	29.9 t	28.5 t	30.0 t	29.9 t
24	78.3 d	79.1 d	78.0 d	79.5 d	78.5 d	79.5 d	79.4 d
25	73.8 s	73.5 s	73.8 s	73.8 s	73.8 s	73.8 s	73.8 s
26	25.4 q	25.1 q	25.4 q	25.1 q	25.4 q	25.1 q	25.1 q
27	25.5 q	25.6 q	25.4 q	25.6 q	25.4 q	25.6 q	25.6 q
28	29.0 q	28.8 q	29.0 q	23.4 q	25.4 q	24.9 q	26.5 q
29	16.0 q	15.8 q	15.9 q	25.3 q	25.2 q	27.2 q	14.8 q
30	21.9 q	20.5 q	23.0 q	28.7 q	26.1 q	68.7 t	18.1 q
1′					56.5 s		

10000 rpm for 10 min. Then supernatants were extracted with EtOAc (1 ml) and analyzed by TLC. Control experiments were conducted in the absence of either CCG or the fungus. Preparative scale biotransformation was performed in 1000 ml Erlenmeyer flasks each containing 300 ml of biotransformation medium using 1080 mg CCG, and incubated at 25 °C, 180 rpm for 10 days. After incubation period, the mycelia were filtered on a Buchner funnel, the combined filtrate was extracted with EtOAc (5.5 L x 2), and the organic phase was dried over anhydrous Na$_2$SO$_4$, followed by filtration and evaporation in vacuo.

4.5. Isolation and purification

After evaporation of the solvent in vacuo, 2.5 g of extract was obtained due to the presence of unconsumed nutrients, as well as undesired metabolic by-products of the fungus. The EtOAc extract (2.5 g) was first chromatographed on a Sephadex-LH 20 column (70 g) and eluted with 100% MeOH, which provided 80 fractions. Fractions 38 to 48 were pooled together for further purification. This fraction (1.90 g) was subjected to a reversed-phase column (C-18, 100 g), using MeOH−H$_2$O (45:55 to 90:10) and 100% MeOH yielding 295 fractions. Fraction 66−80 (78 mg) was submitted to silica gel column (50 g) chromatography with the solvent system CHCl$_3$−MeOH−H$_2$O (90:10:0.5 to 82.5:17.5:0.5) to give 3 subfractions. Subfraction 1 (20 mg) was further purified on a silica gel column (10 g) using cyclohexane-EtOAc-MeOH (10:10:2) to afford metabolite **6** (5 mg). Fraction 94−100 (122 mg) was chromatographed over silica gel column (60 g) with the solvent system CHCl$_3$−MeOH−H$_2$O (90:10:0.5 to 85:15:0.5) to provide **1** (22 mg) and **2** (5.5 mg). Fraction 133−155 (82 mg) was subjected to a silica gel column (15 g), and eluted with CHCl$_3$−MeOH−H$_2$O (90:10:0.5 to 85:15:0.5) to give 8 mg of **4**. Fraction 169−185 (91 mg) was

purified on a silica gel column (50 g) using CHCl$_3$−MeOH−H$_2$O (90:10:0.5 to 85:15:0.5) to give metabolite **3** (22.2 mg). Fraction 186−200 (135 mg) was further fractionated over silica gel column (55 g) with the solvent system CHCl$_3$−MeOH−H$_2$O (90:10:0.5 to 82.5:17.5:0.5) to give 20 mg of metabolite **8**. Fraction 201−210 (84 mg) was chromatographed over silica gel column (50 g) with the solvent system CHCl$_3$−MeOH−H$_2$O (90:10:0.5 to 85:15:0.5) to give 4 subfractions. Subfraction 4 (14 mg) was further purified on silica gel column (10 g) using CHCl$_3$−MeOH−H$_2$O (90:10:0.5 to 85:15:0.5) to afford **7** (6.5 mg). Fraction 285−295 (30 mg) was further applied to a silica gel column (30 g) using CHCl$_3$−MeOH (97.5:2.5 to 90:10) as eluent to purify 8 mg of metabolite **5**.

4.6. Spectral data of **1**−**7**

Metabolite 1: ^{1}H NMR (CD$_3$OD, 400 MHz): see Table 1; ^{13}C NMR (CD$_3$OD, 100 MHz): see Table 2; HR-MS: m/z 531.3664 [M+Na]$^+$ (C$_{30}$H$_{52}$O$_6$Na, calcd. 531.3661).

Metabolite 2: ^{1}H NMR (CD$_3$OD, 400 MHz): see Table 1; ^{13}C NMR (CD$_3$OD, 100 MHz): see Table 2; HR-MS: m/z 531.3679 [M+Na]$^+$ (C$_{30}$H$_{52}$O$_6$Na, calcd. 531.3661).

Metabolite 3: ^{1}H NMR (CD$_3$OD, 400 MHz): see Table 1; ^{13}C NMR (CD$_3$OD, 100 MHz): see Table 2; HR-MS: m/z 531.3672 [M+Na]$^+$ (C$_{30}$H$_{52}$O$_6$Na, calcd. 531.3661).

Metabolite 4: ^{1}H NMR (CD$_3$OD, 400 MHz): see Table 1; ^{13}C NMR (CD$_3$OD, 100 MHz): see Table 2; HR-MS: m/z 525.3206 [M+Na]$^+$ (C$_{30}$H$_{46}$O$_6$Na, calcd. 525.3192).

Metabolite 5: ^{1}H NMR (CD$_3$OD, 400 MHz): see Table 1; ^{13}C NMR (CD$_3$OD, 100 MHz): see Table 2; HR-MS: m/z 525.3566 [M+Na]$^+$ (C$_{31}$H$_{50}$O$_5$Na, calcd. 525.3555).

Metabolite 6: ^{1}H NMR (CD$_3$OD, 400 MHz): see Table 1; ^{13}C NMR (CD$_3$OD, 100 MHz): see Table 2; HR-MS: m/z 527.3370 [M+Na]$^+$ (C$_{30}$H$_{48}$O$_6$Na, calcd. 527.3348).

Metabolite 7: ^{1}H NMR (CD$_3$OD, 400 MHz): see Table 1; ^{13}C NMR (CD$_3$OD, 100 MHz): see Table 2; HR-MS: m/z 529.3522 [M+Na]$^+$ (C$_{30}$H$_{50}$O$_6$Na, calcd. 529.3505).

Appendix A. Supplementary data

Supplementary data related to this article can be found at https://doi.org/10.1016/j.phytochem.2018.04.006.

References

Bedir, E., Kula, C., Öner, Ö., Altaş, M., Tağ, Ö., Öngen, G., 2015. Microbial transformation of *Astragalus* sapogenins using *Cunninghamella blakesleeana* NRRL 1369 and *Glomerella fusarioides* ATCC 9552. J. Mol. Catal. B Enzym 115, 29−34.

Bianchini, L.F., Arruda, M.F.C., Vieira, S.R., Campelo, P.M.S., Gregio, A.M.T., Rosa, E.A.R., 2015. Microbial biotransformation to obtain new antifungals. Front. Microbiol. 6, 1−12.

Borges, K.B., Borges, W.d S., Durán-Patrón, R., Pupo, M.T., Bonato, P.S., Collado, I.G., 2009. Stereoselective biotransformations using fungi as biocatalysts. Tetrahedron Asymmetry 20, 385−397.

Carballeira, J.D., Quezada, M.A., Hoyos, P., Simeó, Y., Hernaiz, M.J., Alcantara, A.R., Sinisterra, J.V., 2009. Microbial cells as catalysts for stereoselective red-ox reactions. Biotechnol. Adv. 27, 686−714.

de Carvalho, C.C.C.R., 2016. Whole cell biocatalysts: essential workers from Nature to the industry. Microb. Biotechnol.

de Carvalho, C.C.C.R., 2011. Enzymatic and whole cell catalysis: finding new strategies for old processes. Biotechnol. Adv. 29, 75−83.

Çalış, İ., Yürüker, A., Taşdemir, D., Wright, A.D., Sticher, O., Luo, Y.D., Pezzuto, J.M., 1997. Cycloartane triterpene glycosides from the roots of *Astragalus*

melanophrurius. Planta Med. 63, 183–186.

Feng, L.M., Ji, S., Qiao, X., Li, Z.W., Lin, X.H., Ye, M., 2015. Biocatalysis of cyclo-astragenol by *Syncephalastrum racemosum* and *Alternaria alternata* to discover anti-aging derivatives. Adv. Synth. Catal. 357, 1928–1940.

Harley, C.B., Khar, S.P., Ramaseshan, M., Ramiya, P., Pirot, Z.Z., Fauce, S., Lin, T., 2010. Compositions and methods for increasing telomerase activity. U. S. Patent 20100292197 A1, November 18, 2010.

Kuban, M., Öngen, G., Bedir, E., 2010. Biotransformation of cycloastragenol by *Cunninghamella blakesleeana* NRRL 1369 resulting in a novel framework. Org. Lett. 12, 4252–4255.

Kuban, M., Öngen, G., Khan, I.A., Bedir, E., 2013. Microbial transformation of cycloastragenol. Phytochemistry 88, 99–104.

Lam, K.S., 2009. Application of whole-cell biotransfotmation in the pharmaceutical industry. In: Tao, J., Lin, G.-Q., Liese, A. (Eds.), Biocatalysis for the Pharmaceutical Industry: Discovery, Development, and Manufacturing. John Wiley & Sons (Asia) Pte Ltd, Singapore, pp. 214–227, 324p.

Lu, L., Chen, J.-C., Song, H.-J., Li, Y., Nian, Y., Qiu, M.-H., 2010. Five new triterpene bisglycosides with acyclic side chains from the rhizomes of *Cimicifuga foetida* L. Chem. Pharm. Bull. (Tokyo) 58, 729–733.

Ludwig-Müller, J., 2015. Plants and endophytes: equal partners in secondary metabolite production? Biotechnol. Lett. 37, 1325–1334.

Nalbantsoy, A., Nesil, T., Erden, S., Çalış, İ., Bedir, E., 2011. Adjuvant effects of *Astragalus* saponins macrophyllosaponin B and astragaloside VII. J. Ethnopharmacol. 134, 897–903.

Özipek, M., Dönmez, A.A., Çalış, İ., Brun, R., Rüedi, P., Tasdemir, D., 2005. Leishma-nicidal cycloartane-type triterpene glycosides from *Astragalus oleifolius*. Phytochemistry 66, 1168–1173.

Pimentel, M.R., Molina, G., Dionísio, A.P., Maróstica Junior, M.R., Pastore, G.M., 2011. The use of endophytes to obtain bioactive compounds and their application in biotransformation process. Biotechnol. Res. Int. 2011, 576286.

Schoch, C.L., Seifert, K.A., Huhndorf, S., Robert, V., Spouge, J.L., Levesque, C.A., Chen, W., Consortium, F.B., 2012. Nuclear ribosomal internal transcribed spacer (ITS) region as a universal DNA barcode marker for Fungi. Proc. Natl. Acad. Sci. 109, 6241–6246.

Shah, S.A.A., Tan, H.L., Sultan, S., Faridz, M.A.B.M., Shah, M.A.B.M., Nurfazilah, S., Hussain, M., 2014. Microbial-catalyzed biotransformation of multifunctional triterpenoids derived from phytonutrients. Int. J. Mol. Sci.

Shaymaa, M.M., Backheet, E.Y., Bayoumi, S.A., Ross, S.A., 2016. New cycloartane saponin and monoterpenoid glucoindole alkaloids from *Mussaenda luteola*. Fitoterapia 110, 129–134.

Tağ, Ö., Çağır, A., Khan, I.A., Bedir, E., 2012. Cleavage of ring A and formation of an unusual nor-triterpene skeleton via the Baeyer-Villiger reaction. Tetrahedron Lett. 53, 5864–5867.

Tao, J., Xu, J.H., 2009. Biocatalysis in development of green pharmaceutical pro-cesses. Curr. Opin. Chem. Biol. 13, 43–50.

Vincken, J.P., Heng, L., de Groot, A., Gruppen, H., 2007. Saponins, classification and occurrence in the plant kingdom. Phytochemistry 68, 275–297.

Wang, Y., Dai, C.C., 2011. Endophytes: a potential resource for biosynthesis, biotransformation, and biodegradation. Ann. Microbiol. 61, 207–215.

Woudenberg, J.H.C., Groenewald, J.Z., Binder, M., Crous, P.W., 2013. Alternaria redefined. Stud. Mycol. 75, 171–212.

Yang, W.Z., Ye, M., Huang, F.X., He, W.N., Guo, D.A., 2012. Biocatalysis of cyclo-astragenol by filamentous fungi to produce unexpected triterpenes. Adv. Synth. Catal. 354, 527–539.

Yoshikawa, K., Katsuta, S., Mizumori, J., Arihara, S., 2000. Four cycloartane tri-terpenoids and six related saponins from *Passiflora edulis*. J. Nat. Prod. 63, 1229–1234.